J|A|C|S COMMUNICATIONS

Published on Web 01/11/2010

# Maze Solving by Chemotactic Droplets

István Lagzi,[†] Siowling Soh,[†] Paul J. Wesson,[†] Kevin P. Browne,[‡] and Bartosz A. Grzybowski*[,†,‡]

*Department of Chemical and Biological Engineering and Department of Chemistry, Northwestern University, 2145 Sheridan Road, Evanston, Illinois 60208-3113*

Received September 22, 2009; E-mail: grzybor@northwestern.edu

Solving maze problems is not only relevant to the everyday issues of urban transportation[1] and to experimental psychology[2] but is also one of the model problems of network and graph theory[3] as well as robotics.[4] With the advent of computers, algorithms for maze solving have become automated, but the solution times still scale unfavorably with maze size/complexity.[5] Several groups have thus explored the possibility of maze solving by physical, chemical, or even biological systems: microfluidic networks,[6] chemical waves[7] or plasmas,[8] or microorganisms growing in response to food gradients within the maze.[9] Inspired by the latter example, we wished to create a system in which an inanimate/chemical construct would be self-propelled and solve mazes in response to chemical stimuli. Here we describe one such system comprising small droplets powered by the combination of acid/base chemistry and surface tension effects. When subject to a pH gradient within a maze, these droplets move toward regions of low pH and find the shortest of multiple possible paths. Taxis in our system is over distances of several centimeters and derives from the convection flows developed outside of the droplets.[10]

The templates for the mazes were fabricated by conventional photolithography in SU-8 photoresist (SU8-100, Microchem) and were subsequently replicated into poly(dimethyl siloxane) (PDMS, Sylgard 184, Dow Corning). The channels of the maze were 1.4 mm wide and 1.0 mm tall and were filled with 240 $\mu$L of aqueous KOH solution (pH 12.0−12.3) with surfactant added to reduce surface tension. A small block of high gel strength agarose (EMD Chemicals) soaked in a solution of HCl (pH 1.2) was placed at one entrance of the maze. After a time $t$ of 30−40 s (the minimum time required to set up pH gradients through the maze), a small droplet (∼1 $\mu$L) of an organic solvent immiscible with water [typically mineral oil (MO) or dichloromethane (DCM)] and containing 20−60% (v/v) of 2-hexyldecanoic acid (HDA) was placed at the other entrance to the maze. To increase the optical contrast, the droplet was dyed with Calco Oil Red (American Cyanamid).

Once in the maze, the droplet moved toward the regions of lower pH, that is, toward the source of HCl. In doing so, it always found the shortest path through the maze, although the details of this process depended on the composition of the drop. HDA/DCM droplets moved rapidly (up to ∼10 mm s$^{-1}$) and, because of their high inertia, sometimes veered off onto the wrong path, from which, however, they rapidly reverted to the optimal one [Figure 1a,b; also see videos 1 and 2 in the Supporting Information (SI)]. In contrast, droplets of HDA in mineral oil moved slowly (∼1 mm s$^{-1}$) but migrated smoothly along the shortest path. The difference in the rate of motion could be due to the difference in partition coefficients of HDA between the phases (mineral oil/KOH solution vs DCM/KOH solution), which can affect the rates of HDA release from the droplets. We emphasize that in all of these experiments, the presence of both HDA and the pH gradient was crucial to the droplet's "chemotaxis": when the droplets lacked HDA or when the pH was uniform throughout the maze, no directional motion of the droplets was observed.[12]

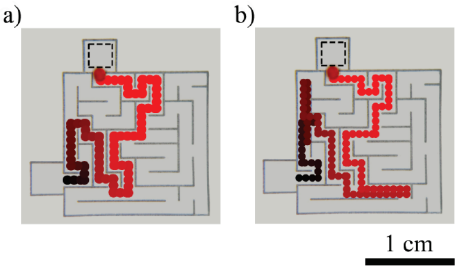


***Figure 1.*** Maze solving by chemotactic droplets [here, 1 $\mu$L droplets of 20% (v/v) HDA in DCM]. In (a), the droplet moved straight to the exit along the shortest path. In (b), the droplet went astray at two locations but corrected its trajectory and ultimately found the shortest path. The images were created by overlaying experimental images at different times. Color coding corresponds to time: dark violet, early times; red, later times. The position of the gel soaked with HCl at the maze's entrance is indicated by dashed-line boxes. Videos 1 and 2 corresponding to these images are included in the SI.

Maze solving by HDA-containing drops can be explained by surface tension effects stemming from the nonuniform distribution of HDA at the liquid−air interface (Figure 2). As HDA diffuses from the droplet, it partially deprotonates in the pH gradient. Importantly, more protonated HDA is found in the direction facing the source of acid (i.e., toward lower pH). This asymmetric distribution translates into a gradient of surface tension that is determined predominantly by the concentration of the protonated HDA at the liquid−air interface (deprotonated HDA is much less surface-active; see ref 13). The surface tension gradients in turn give rise to convective flows,[14] which are ultimately responsible for particle motion. In this context, it should be noted that although there are Marangoni-like flows inside of the droplet, their velocities (∼0.1 mm s$^{-1}$) are too small to account for droplet's translation with the experimentally observed velocities.

The above, qualitative description can be formalized in the form of Navier−Stokes (NS) equations describing the fluid dynamics of the system. Consider the model geometry illustrated in Figure 2a, where the HDA droplet is in the middle of a channel and the acid-soaked gel is at one end of the channel. The conservation equation for HDA can be written as $\mathbf{v}\cdot\nabla c = D\nabla^2 c - k_B c$, where $\mathbf{v}$ is the velocity of the liquid, $c$ is the concentration of HDA, $D$ is its diffusion coefficient, and $k_B$ is the rate of consumption of HDA by the basic solution. Since the amount of HDA emitted by the droplet is small (∼$10^{-3}$ $\mu$L min$^{-1}$, estimated by monitoring the droplet size as a function of time), the equation assumes a quasi-steady-state approximation.[15] The boundary condition on the side of the domain where the acidic gel is present can be expressed as $-D\nabla c = \mathbf{J}_{gel}$,

[†] Department of Chemical and Biological Engineering.
[‡] Department of Chemistry.



10.1021/ja9076793 

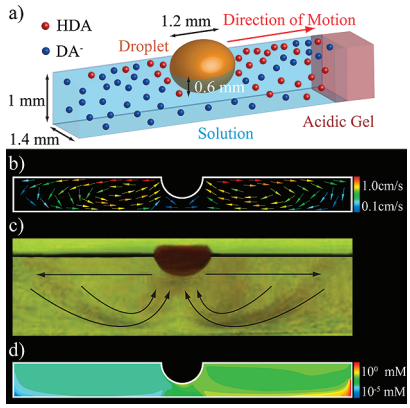


***Figure 2.*** (a) Scheme of a droplet in a channel. The presence of HDA at the liquid−air interface gives rise to convective flows. Since more HDA is present in the direction facing the source of acid, the flows and forces are asymmetric. (b) Velocity field based on the theoretical model described in the main text (calculated using the Fluent computational fluid dynamics package from Ansys). (c) Experimental image of the convection rolls visualized using Neutral Red indicator (see also video 3 in the SI). (d) Numerical solution of the concentration profile of HDA in solution. The profile shows asymmetry (more HDA on the "right" side of the droplet facing the source of HCl than on the "left" side), which explains the motion of the droplet toward the acidic gel.

where $\mathbf{J}_{gel}$ is the flux of HDA out of this boundary into the solution. The boundary of the droplet is assumed to emit a constant flux of HDA, i.e., $-D\nabla c = \mathbf{J}_{droplet}$. No-flux and no-slip conditions are assumed for all of the other boundaries (the no-slip boundary condition can be assumed since the fluid velocity inside the droplet is ~0.1 mm $s^{-1}$, i.e., 2−3 orders of magnitude lower than that outside the droplet). These conditions are coupled with the NS equation, which governs the convective flows in the liquid: $\rho\mathbf{v}\cdot\nabla\mathbf{v} = -\nabla P + \mu\nabla^2\mathbf{v}$, where $\rho$ is the density of the liquid, $\mu$ is the viscosity, and $P$ is the pressure. At the liquid−air interface, shear stress is generated by the gradients $\tau_{xy} = \mu(\partial v_x/\partial y) = \partial\gamma/\partial x$, where $\gamma$ is the surface tension. In the dilute approximation, which is applicable at the micromolar concentrations used here, the relationship between surface tension and HDA concentration is linear:[16] $\gamma = \gamma_0 - bc$, where $\gamma_0$ is the surface tension of pure water and $b$ is a constant of proportionality. With the parameter values $D = 10^{-9}$ $m^2$ $s^{-1}$, $k_B = 1$ $s^{-1}$, $|\mathbf{J}_{droplet}| = 10^{-5}$ mol $m^{-2}$ $s^{-1}$, $|\mathbf{J}_{gel}| = 10^{-3}$ mol $m^{-2}$ $s^{-1}$, and $b = 0.05$ N $m^2$ $mol^{-1}$ (see ref 17 and also section 3 in the SI), the system of NS equations can be solved numerically.

Figure 2b shows the calculated velocity vector field in the liquid, where the flows form two convection rolls, one on each side of the droplet. Such rolls were also observed in the experiments (Figure 2c), and the calculated and experimentally measured fluid velocities were both on the order of centimeters per second. Importantly, the concentration gradients of HDA are steeper in the direction facing the source of acid (to the "right" in Figure 2d), and consequently, the fluid velocities are also higher in this direction. By Bernoulli's principle [applicable because the Reynolds numbers for the system are $Re \sim O(10^3)$], higher velocities translate into a lower pressure and a net force, $F_{net}$, that originates from the sum of two major contributions integrated over the particle's surface: (i) pressure forces, $F_{press} = \int P\,dy$, and (ii) viscous drag forces due to shear stresses, $F_{vis} = \int\mu(\partial v_x/\partial y)\,dx$. Overall, $F_{net}$ is directed toward the acidic gel, and its value is ~$6 \times 10^{-9}$ N. When the droplet starts moving, it also experiences a viscous drag force, $F_v$, which counteracts $F_{net}$. At steady state, $F_{net} = F_v = 3\pi R\mu v_{ss}$, where $R \approx 0.6$ mm is the radius of the droplet and $v_{ss}$ is the steady-state velocity. This gives $v_{ss} \approx 1$ mm $s^{-1}$, which is close to the experimental velocities of the droplets in the maze. Although the model we developed is simplified (e.g., by not taking into account the actual geometry of the maze), it captures the essence of the maze solving, namely, that wherever a pH difference exists around the droplet emitting the surface-active chemical, this difference translates into chemotaxis of the droplet. This property suggests that chemicals other than those we used here can be used to construct chemotactic chemical systems. On the other hand, it must be remembered that in mazes significantly larger than those used here, the times to establish the pH gradients will be significantly longer, and these gradients might also be of comparable "steepness" along different paths, leading to more "errors" during droplet navigation.

**Acknowledgment.** This work was supported by the DARPA Program (01-130130-00//W911NF-08-1-0143) and the Nonequilibrium Energy Research Center, which is an Energy Frontier Research Center funded by the U.S. Department of Energy, Office of Science, Office of Basic Energy Sciences under Award DE-SC0000989.

**Supporting Information Available:** Experimental and numerical details and five video files (AVI). This material is available free of charge via the Internet at http://pubs.acs.org.

## References

(1) Modesti, P.; Sciomachen, A. *Eur. J. Oper. Res.* **1998**, *111*, 495.
(2) Crowe, D. A.; Averbeck, B. B.; Chafee, M. V.; Anderson, J. H.; Georgopoulos, A. P. *J. Cognit. Neurosci.* **2000**, *12*, 813.
(3) (a) Teroa, A.; Kobayashia, R.; Nakagaki, T. *Physica A* **2006**, *363*, 115. (b) Adamatzky, A. I. *Math. Comput. Model.* **1996**, *23*, 105.
(4) Rao, N. S. V.; Kareti, S.; Shi, W.; Iyengar, S. S. *Robot Navigation in Unknown Terrains: Introductory Survey of Non-Heuristic Algorithms*; Oak Ridge National Laboratory Technical Report: Oak Ridge, TN, 1993.
(5) Dijkstra, E. W. *Numer. Math.* **1959**, *1*, 269.
(6) Fuerstman, M. J.; Deschatelets, P.; Kane, R.; Schwartz, A.; Kenis, P. J. A.; Deutch, J. M.; Whitesides, G. M. *Langmuir* **2003**, *19*, 4714.
(7) Steinbock, O.; Tóth, Á.; Showalter, K. *Science* **1995**, *267*, 868.
(8) Reyes, D. R.; Ghanem, M. M.; Whitesides, G. M.; Manz, A. *Lab Chip* **2002**, *2*, 113.
(9) (a) Nagakaki, T.; Yamada, H.; Tóth, Á. *Nature* **2000**, *407*, 470. (b) Nagakaki, T.; Yamada, H.; Tóth, Á. *Biophys. Chem.* **2001**, *92*, 47.
(10) In a recent study by Sugawara (see ref 11), oil droplets containing a fatty acid anhydride and immersed in a solution of fatty acid micelles were shown to exhibit taxis toward regions of high pH. In this system, however, the convection flows were localized inside of the droplets, and the distances of tactic motion were on the order of 100 $\mu$m. We also note that the directionality of motion predicted by the model and observed in our experiments is opposite to the behavior of Sugawara's system (see section 1 in the SI).
(11) (a) Hanczyc, M. M.; Toyota, T.; Ikegami, T.; Packard, N.; Sugawara, T. *J. Am. Chem. Soc.* **2007**, *129*, 9386. (b) Matsumo, H.; Hanczyc, M. M.; Ikegami, T. *Lect. Notes Comp. Sci.* **2007**, *4828*, 179.
(12) We also performed experiments with multiple droplets placed into the maze either simultaneously or sequentially (at different time intervals). In all cases, the droplets found the optimal path, indicating that their trajectories were determined by the pH gradient and not, for instance, by interactions between droplets (also see section 2 and videos 4 and 5 in the SI).
(13) (a) Fainerman, V. B.; Miller, R.; Aksenenko, E. V.; Makievski, A. V. In *Surfactants: Chemistry, Interfacial Properties, Applications*; Fainerman, V. B., Möbius, D., Miller, R., Eds.; Elsevier: Amsterdam, 2001; pp 189−285. (b) Lucassen, E. *J. Colloid Interface Sci.* **1972**, *41*, 156.
(14) Soh, S.; Bishop, K. J. M.; Grzybowski, B. A. *J. Phys. Chem. B* **2008**, *112*, 10848.
(15) Bodenstein, M. *Z. Phys. Chem.* **1913**, *85*, 329.
(16) Adamson, A. W. *Physical Chemistry of Surfaces*, 5th ed.; John Wiley & Sons: New York, 1990.
(17) Deen, W. M. *Analysis of Transport Phenomena*; Oxford University Press: New York, 1998.

JA9076793